doi:10.1016/j.jmb.2009.04.085 J. Mol. Biol. (2009) 391, 12–25

JMB

Available online at www.sciencedirect.com

ScienceDirect

ELSEVIER

Chromatin Remodelers Act Globally, Sequence Positions Nucleosomes Locally

Peretz D. Partensky[1,2] and Geeta J. Narlikar[2]*

[1]*Biophysics Graduate Group, University of California, San Francisco, CA 94158, USA*

[2]*Department of Biochemistry and Biophysics, University of California, San Francisco, CA 94158, USA*

Received 6 January 2009; received in revised form 19 April 2009; accepted 30 April 2009
Available online 18 May 2009

The precise placement of nucleosomes has large regulatory effects on gene expression. Recent work suggests that nucleosome placement is regulated in part by the affinity of the underlying DNA sequence for the histone octamer. Nucleosome locations are also regulated by several different ATP-dependent chromatin remodeling enzymes. This raises the question of whether DNA sequence influences the activity of chromatin remodeling enzymes. DNA sequence could most simply regulate nucleosome remodeling through its effect on nucleosome stability. In such a model, unstable nucleosomes would be remodeled faster than stable nucleosomes. It is also possible that certain DNA elements could regulate remodeling by inhibiting the interaction of nucleosomes with the remodeling enzyme. A third possibility is that DNA sequence could regulate the outcome of remodeling by influencing how reaction intermediates collapse into a particular set of stable nucleosomal positions. Here we dissect the contribution from these potential mechanisms to the activities of yeast RSC and human ACF, which are representative members of two major classes of remodeling complexes. We find that varying the histone–DNA affinity over 3 orders of magnitude has negligible effects on the rates of nucleosome remodeling and ATP hydrolysis by these two enzymes. This suggests that the rate-limiting step for nucleosome remodeling may not involve the disruption of histone–DNA contacts. We further find that a specific curved DNA element previously hypothesized to inhibit ACF activity does not inhibit substrate binding or remodeling by ACF. The element, however, does influence the distribution of nucleosome positions generated by ACF. Our data support a model in which remodeling enzymes move nucleosomes to new locations by a general sequence-independent mechanism. However, consequent to the rate-limiting remodeling step, the local DNA sequence promotes a collapse of remodeling intermediates into highly resolved positions that are dictated by thermodynamic differences between adjacent positions.

Keywords: nucleosome positioning; histone–DNA affinity; chromatin remodeling; human ACF; RSC

Edited by J. O. Thomas

Introduction

The eukaryotic genome is packaged by wrapping ~147-bp units of DNA around histone octamers to form chains of nucleosomes. The packaging of the DNA within a nucleosome reduces access of the DNA to most transcription factors and polymerases. In between nucleosomes, there are regions of more accessible DNA, called linker regions, which vary from a few base pairs to several hundred base pairs.[1] Thus, within any given cell type, the precise partitioning of the genome into nucleosome-bound and nucleosome-free DNA regions can have large consequences on gene regulation and help define a particular cellular state.[2]

Recent studies suggest that the genome plays a large role in encoding its own packaging through differences in affinity of the underlying sequence for the histone octamer (Fig. 1a).[3] Genome-wide nucleosome mapping studies have found that ~80% of all yeast nucleosomes adopt specific positions.[1,3–5] The nucleosome positions are often predicted from the

*Corresponding author. E-mail address: geeta.narlikar@ucsf.edu.

Abbreviation used: FRET, fluorescence resonance energy transfer.

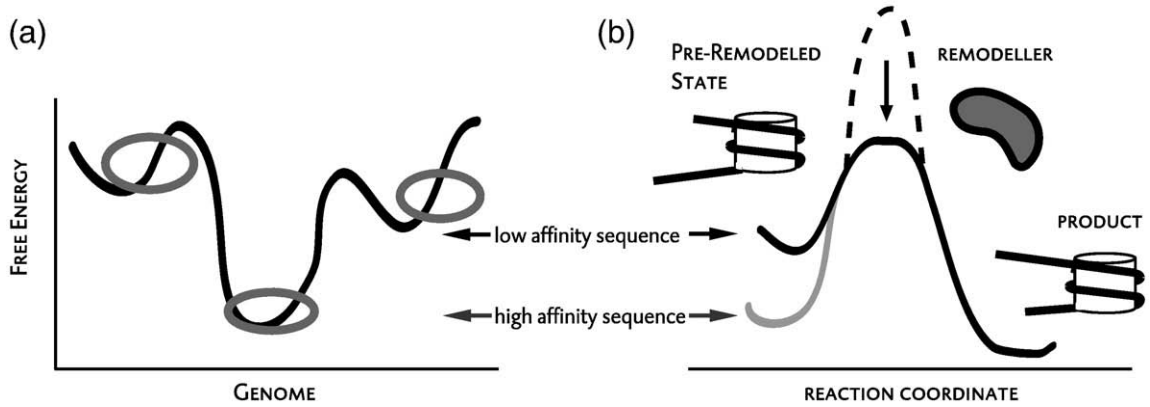

Fig. 1. Model: chromatin remodeling enzymes help nucleosomes equilibrate on the genomic thermodynamic landscape. (a) A schematic of a thermodynamic landscape representing differences in the free energy of interaction between DNA and the histone octamer. Nucleosomes are thought to equilibrate on this energy landscape with the assistance of remodeling enzymes. (b) One model for how histone–DNA affinity regulates the activity of remodeling enzymes. In the absence of remodeling enzyme, a high-energy barrier (dashed line) kinetically traps nucleosomes in nonequilibrium locations. A remodeling enzyme promotes rapid equilibration by lowering this energetic barrier (solid lines). A prediction of this model is that if we could destabilize the pre-remodeled state, the remodeler would move the nucleosome with a faster rate. Key alternative models are presented in the main text.

primary DNA sequence based on the ability of the DNA sequence to bend in a manner required for nucleosome formation.[6,7] Other work has mapped local changes in nucleosome positions in promoter regions across the yeast genome upon environmental stress such as heat shock.[2] These changes in nucleosome positions alter the accessibility of promoter regions to transcription factors. Since such changes in nucleosome positions are generally thought to accompany cellular differentiation and adaptation, it is of interest to understand to what extent and how DNA sequence influences transitions between different chromatin states.

While nucleosomes can assemble on any sequence, under physiological conditions, most nucleosomes do not move on their own,[8] but remain kinetically trapped in their locations. *In vivo*, transitions between chromatin states are catalyzed by ATP-dependent chromatin remodeling machines that rapidly reorganize histone–DNA contacts.[9–12] Thus, understanding whether DNA sequence affects the activity of remodeling enzymes is a key aspect of understanding how DNA sequence might influence transitions between different chromatin states.

One way in which DNA sequence can regulate remodeling activity is by affecting the stability of a nucleosome. This model draws on previous observations that nucleosomes assembled on strong positioning sequences are thermally repositioned more slowly than nucleosomes on weak positioning sequences.[8,13,14] If the rate-limiting transition state for remodeling primarily involves loosened histone–DNA contacts, then remodeling enzymes, like heat, will also move unstable nucleosomes more readily than stable nucleosomes. In such a mechanism, the main function of a remodeling enzyme would be to catalyze rapid equilibration between different nucleosome positions (Fig. 1b). This model predicts that remodeling enzymes will move nucleosomes occupying high-affinity DNA sequences more slowly than nucleosomes occupying lower-affinity DNA sequences. Another recently proposed possibility is that certain DNA sequences adopt topological properties within nucleosomes that inhibit binding by chromatin remodeling complexes and thereby help stabilize nucleosomes in specific locations.[15] While some biochemical studies have shown that ATP-dependent remodeling enzymes can move nucleosomes away from strong nucleosome-positioning sequences,[16–19] other studies suggest that nucleosome-positioning properties of the DNA do play an important role in determining the locations of remodeled nucleosomes.[14,20] These observations have suggested a third model in which DNA sequence does not directly affect the activity of remodeling enzymes, but instead more locally regulates the outcome of remodeling by influencing the collapse of remodeling intermediates into a particular set of stable nucleosomal positions.[14]

To distinguish amongst the three models, we separately measured the effects of nucleosome stability and DNA structure on nucleosome remodeling rates. We tested the activities of two major classes of ATP-dependent remodeling complexes, the ISWI class and the SWI/SNF class, on nucleosomes with different stabilities. These two classes of complexes are highly abundant, act broadly at a number of different loci, and generate substantially different products. We therefore reasoned that results with these two classes would lead to generalizable principles of how DNA sequence influences ATP-dependent nucleosome reorganization. We chose yeast RSC as a representative member of the SWI/SNF class and human ACF as a representative member of the ISWI class. Surprisingly, we find that the rates of nucleosome movement by these complexes are insensitive to 1000-fold changes in histone–DNA affinity. These and other results presented here support the model that DNA sequence regulates ATP-dependent remodeling by

locally influencing the final nucleosome positions adopted by remodeling intermediates.

Results

To determine how DNA sequence regulates the activity of remodeling complexes, we took two complementary approaches. In the first approach, we measured whether changing the stability of nucleosomes by changing DNA sequence affected the remodeling rates of ACF and RSC. In the second approach, we tested whether the introduction of a specific curved DNA element inhibits remodeling by ACF.

Characterization of nucleosomes assembled on four different DNA sequences

We selected four different DNA sequences as our experimental inputs, designated as 601,[21] TPT,[22] 5S,[23] and ARB.[18] The first, 601, is a synthetically selected positioning sequence. It has amongst the highest known affinities for the histone octamer and is commonly used as an experimental tool in nucleosome-based assays because of its strong ability to position nucleosomes *in vitro*. TPT is another previously used, synthetically derived positioning sequence. 5S is a naturally occurring nucleosome positioning sequence that has commonly been used to position nucleosomes *in vitro*. ARB is a sequence arbitrarily chosen from a bacterial plasmid that we have used previously.[18]

We used two approaches to measure differences in affinity amongst the test sequences for the histone octamer (Fig. 2). In the first approach, we used a competitive nucleosome assembly method developed previously.[21,24–26] In this method, a tracer amount of a specific sequence competes with a large amount of a background DNA sequence for a limiting amount of histone octamer. The tracer sequence is fluorescently labeled, while the background sequence is unlabeled. Comparing the fraction of tracer DNA incorporated into nucleosomes for the different sequences then allows calculation of the relative free energies for nucleosome assembly (see Materials and Methods for more details). We visualized the tracer DNA by end-labeling it with Cy3. To ensure we were measuring the energetics of a specific nucleosome position, our competition experiment was done on 147-bp core segments of DNA. Using this approach, we found that our sequences vary in affinity for the histone octamer over several hundred fold, representing a

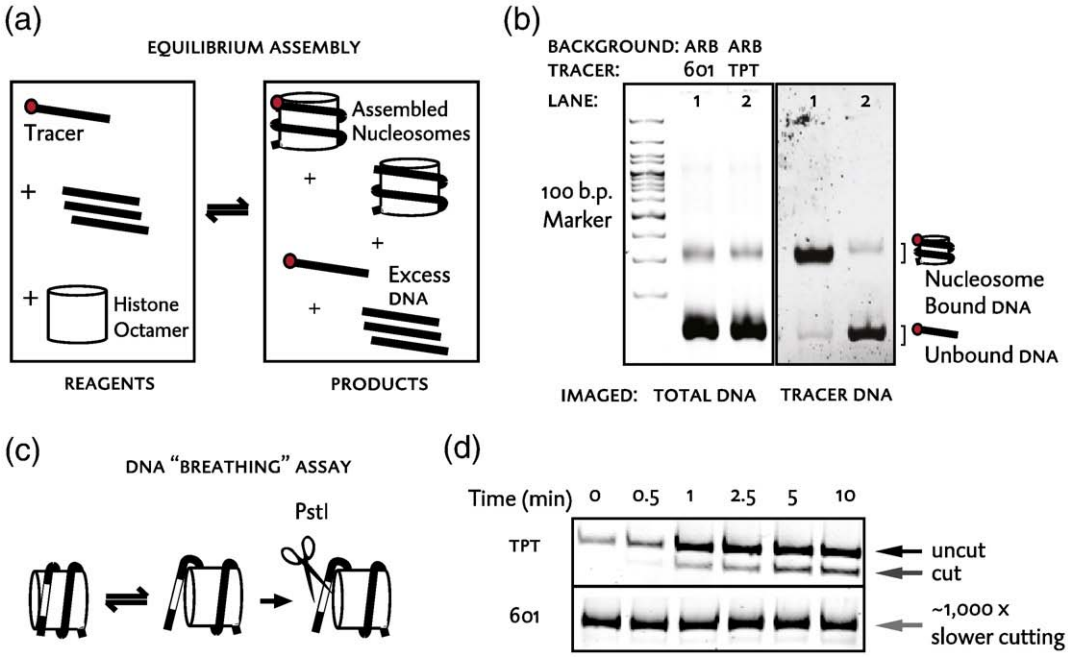

Fig. 2. Characterization of nucleosomes assembled on different sequences. (a) Excess background DNA (40 μg) and tracer amount of the 147-bp test sequence (<100 ng) were assembled on a limiting quantity of histone octamer (3 μg) in a 60 uL reaction. (b) Representative native gel of competitive assembly products. Left, shows that the same total quantity of DNA is assembled into nucleosomes in both lanes, independent of tracer. Right, shows the fluorescently labeled tracer in the same two lanes. The 601 sequence (lane 1) has much higher affinity for the nucleosome than the TPT sequence (lane 2) in the context of the competitor DNA. See Table 1 for quantification. (c) A PstI restriction enzyme site was incorporated ~18 bp inside core nucleosomes assembled on 147-bp of DNA. Previous work has shown that nucleosomal DNA transiently unravels from the histone octamer and becomes accessible to cutting by restriction enzymes. To determine how DNA sequence affects this unraveling, the rate of cutting by PstI (10 U/μl) was measured. (d) Representative time courses of restriction enzyme accessibility reactions. Comparison of the top and bottom panels shows that in the context of the 601 sequence the PstI site becomes accessible almost 1000-fold more slowly than in the context of TPT. See Table 1 for quantification.

3.0 kcal/mol range in the free-energy differences at 4 °C (Table 1, $\Delta\Delta G_{ARB}$). The free-energy difference that we obtain between 601 and 5S agrees well with previous measurements.[27] Furthermore, the range of free-energy differences covered by our test sequences is comparable to the maximal range seen *in vitro*[8] and substantially larger than the variability in affinity observed *in vivo*.[26]

In the second approach, we measured differences in the propensity of the DNA sequences to transiently unravel from the histone octamer. We used this additional approach for the following reasons. Nucleosomal DNA can spend as much as 10% of its time away from the octamer and exposed to solution and it has therefore been proposed that capturing unraveled nucleosomal DNA may be an early step in ATP-dependent chromatin remodeling.[28–30] Further, the free energy required to unravel the same amount of DNA can vary by as much as ~7.3 kcal/mol depending on sequence, raising the possibility that sequence may regulate remodeling through effects on DNA unraveling.[31] As described previously, the equilibrium between the unraveled and bound states of DNA can be obtained from the rate of restriction enzyme cutting at a restriction site within a nucleosome[31] (see Materials and Methods). We engineered a PstI site at the same location (~18 bp in from one end) within all four test sequences. Further, as with the competitive assembly experiments, we assembled nucleosomes on 147-bp sequences. By comparing the rates of cutting across the four sequences, we found that the propensity to expose the PstI site varied by ~1000-fold (~4 kcal/mol at 37 °C) (Fig. 2c and d and Table 1).

Nucleosomes assembled on these sequences represent quantitatively different energy barriers for disruption of histone–DNA interactions and were consequently used as tools to investigate the reaction mechanisms of chromatin remodeling enzymes ACF and RSC.

Rates of remodeling are insensitive to affinity of DNA sequence for histone octamer

To measure the rates of remodeling, we used a previously developed fluorescence resonance energy transfer (FRET)-based technique[18] that allows detection of nucleosome movement in real time (Fig. 3a). We assembled nucleosomes on the four test sequences with 60 bp of flanking DNA. The DNA was end-labeled with the FRET donor Cy3, and histone H2A was labeled with Cy5 at residue 120. This design gives the maximal FRET value when a nucleosome is positioned on one end of the DNA, and any FRET decrease accompanying translational movements of up to 15 bp away from this end position is easily detectable.[18] Due to the strong positioning power of 601, nucleosomes assemble readily on the end of the 601 sequence with 60 flanking base pairs, corresponding to the maximal FRET position. Since weaker affinity sequences are also inherently weaker positioning sequences, for the rest of the sequences, we enriched the end-positioned nucleosomal population through glycerol gradient purification. The 5S sequence with 60 flanking base pairs, however, reequilibrates away from the end position on the time scale of purification and gives rise to a higher variability of the FRET signal due to heterogeneity in the starting material. Therefore, as described below, for nucleosomes assembled on the 5S sequence, we cross-validated our FRET-based results using independent gel-based assays.

To isolate effects of nucleosome stability on the maximal rates of remodeling, the remodeling reactions were carried out with excess and saturating remodeling enzyme. These conditions were also chosen to mimic the *in vivo* conditions where the effective concentration of the remodeler is increased by specific recruitment.

On short stretches of DNA, ACF moves nucleosomes from end positions to centered positions that contain approximately equal flanking DNA on either side.[32,33] Using changes in FRET to measure ACF-catalyzed nucleosome movement, we find that ACF remodels all four nucleosomes with comparable rate constants (Fig. 3c). Thus, the ACF nucleosome remodeling rate is insensitive to large changes in nucleosome stability. As described above, the initial positions of 5S nucleosomes are more heterogeneous and therefore result in a more variable FRET signal. To control for this variability, we also compared the rates of remodeling, using a gel-based assay that allows direct visualization of the final centered product. Centered nucleosomes migrate more slowly through a polyacrylamide gel

Table 1. Quantitative measurements of nucleosomes assembled on different sequences

	Thermodynamic properties		Remodeling activity		ATPase (P_i/enzyme)[a]	
	$\Delta\Delta G_{ARB}$ (assembly) (kcal/mol±SEM)[b]	$\Delta\Delta G_{ARB}$ (breathing) (kcal/mol)[c]	ACF k_{obs} (min^{-1})	RSC k_{obs} (min^{-1})	ACF k_{ATP} (min^{-1})	RSC k_{ATP} (min^{-1})
ARB	0.0[d]	0.0±0.18	1.2±0.2	2.4±0.8	0.21±0.03	4.6±0.3
5S	−0.15±0.05	0.27±0.35	1.1±0.2	N/A	0.34±0.06	7.7±1.0
TPT	−0.22±0.04	0.23±0.20	1.3±0.3	2.8±0.1	0.58±0.08	8.3±1.1
601	−2.98±0.18	−4.19±0.29	1.4±0.1	2.7±0.3	0.49±0.09	6.2±0.6

N/A, not applicable.
[a] Using 4 μM subsaturating ATP and saturating nucleosomes. See Materials and Methods.
[b] ±SEM. See Materials and Methods for full details and fit *R* values.
[c] $\Delta\Delta G$ of PstI site exposure, relative to ARB assembled nucleosome.
[d] ARB is used for reference so defined as 0.

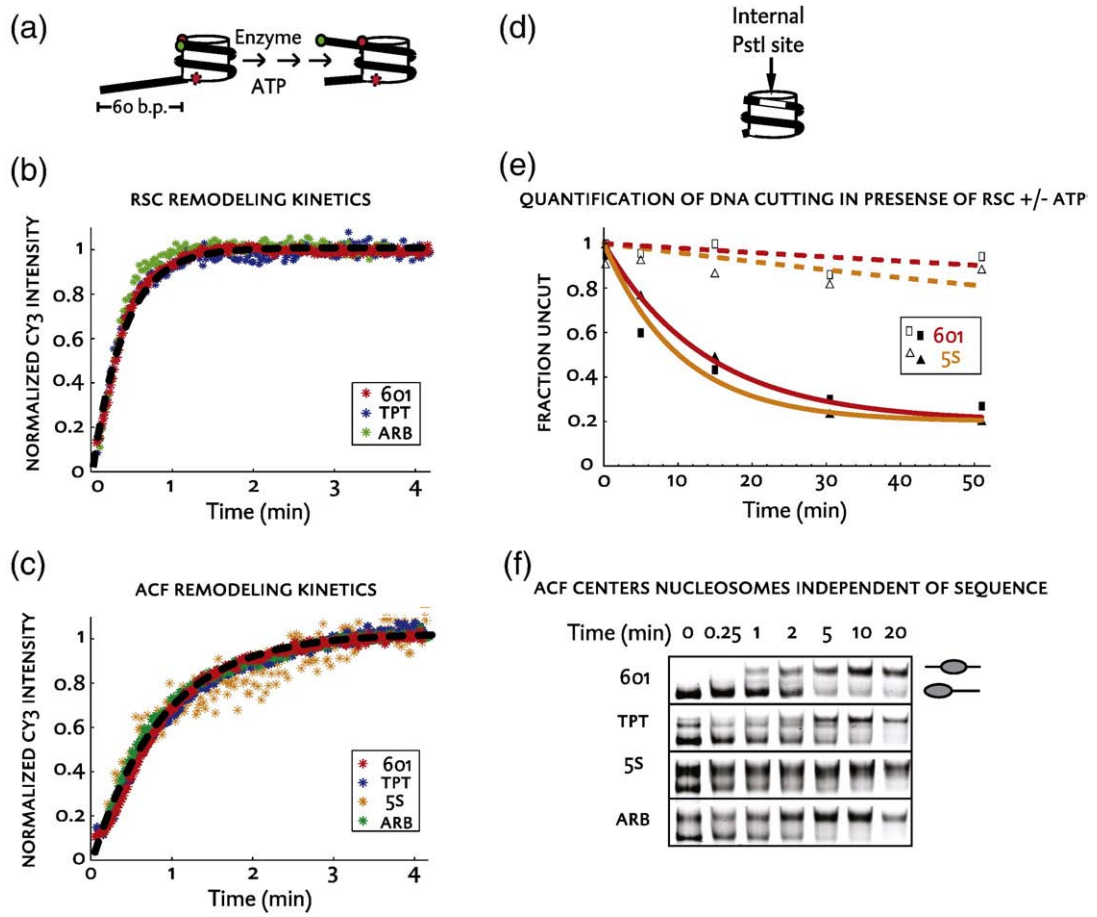

Fig. 3. Chromatin remodelers ACF and RSC displace nucleosomes from high-affinity sequences at similar rates as low-affinity sequences. (a) Schematic of nucleosome structure with Cy5 dye (red) attached to the nucleosome and Cy3 dye (green) attached to the short flanking DNA end. Nucleosomes were assembled on four different sequences of 207-bp length and only the end positions were isolated for the FRET assay, leaving 60 bp of flanking DNA. (b and c) Kinetics of remodeling of the nucleosome constructs by RSC and ACF, respectively, as measured by Cy3 unquenching. A single fit of the average data is included to indicate agreement in remodeling rates between constructs. See Table 1 for quantification of individual reactions. (d) Restriction enzyme accessibility (REA) assay for 601 and 5S sequences. Nucleosomes were assembled on core length sequences of 147 bp such that the PstI site was positioned 18 bp into the nucleosome. During remodeling, RSC destabilizes contacts between the histones and DNA and thereby makes the PstI site accessible to cleavage. This experiment is done at PstI concentrations (0.2 U/μl) lower than that used in the experiment in Fig. 2. (e) Quantification of RSC remodeling by REA assay. Rates are similar for 5S and 601 core nucleosomes. Half-times are 7.6±1.6 and 8.3±1.1 min for 601 and 5S, respectively. Squares and triangles represent 601 and 5S sequences, respectively, while continuous *versus* empty shapes represent presence or absence of ATP. (f) ACF remodeling verified with gel-based assay. Centered nucleosomes migrate more slowly though the gel matrix and appear as an "upshifted" band. ACF moves nucleosomes to central positions independent of sequence. The half-times in minutes for the 601, TPT, 5S and ARB reactions are 2.1, 2.3, 5.2 and 2.6, respectively.

and appear as an accumulation of a higher band in the course of an ACF-remodeling reaction.[18] Time courses of remodeling showed similar rates of movement to the centered position for all nucleosome constructs (see legend to Fig. 3f for quantification). This result also showed that the final remodeled state for all sequences was dominated by the nucleosome-centering mechanism of ACF.

RSC remodels nucleosomes by generating a variety of nucleosomal products that include repositioned nucleosomes and nucleosomes with altered structures.[11] Many of these remodeled products involve displacement of the nucleosome away from its starting position on the DNA and are therefore expected to result in reduced FRET. We used changes in FRET to measure RSC-catalyzed nucleosome movement and found that RSC remodels three of the constructs with comparable rate constants (Fig. 3b). The heterogeneity in the initial positions of 5S nucleosomes combined with the heterogeneity of RSC products prevented us from using FRET to accurately measure remodeling for the 5S nucleosome, presumably because some products resulted in increased FRET, while others resulted in decreased FRET. We, therefore, instead assembled nucleosomes on core segments of the 5S and the 601 sequences to ensure a unique starting position and compared RSC remodeling using a gel-based restriction enzyme accessibility assay. It has previously been shown that at low concentrations of the

restriction enzyme PstI (0.2 U/μl), a nucleosomal PstI site is cut very slowly in the absence of remodeling, but is cut up to 1000-fold faster in the presence of remodeling enzyme and ATP.[34] In these assays, the rate of cutting by PstI reflects the rate of remodeling by the remodeling complex. Using this approach, we found that the rate of remodeling was the same for the high-affinity 601 as the ~3 kcal/mol lower-affinity 5S sequence (Fig. 3b and e).

In summary, by using two independent assays, we found that both ACF and RSC remodel all tested nucleosomes at similar rates. Significantly, the minor differences in the rates show no correlation with the relative stabilities of the nucleosomes (Fig. 3 and Table 1).

Rate of ATP hydrolysis is insensitive to affinity of sequence for histone octamer

The observed insensitivity of remodeling rates to DNA sequence can arise if the remodeling enzymes compensate by hydrolyzing more ATP to remodel the more stable nucleosomes. To test this possibility, we measured the initial rates of ATP hydrolysis by ACF and RSC with each of the four nucleosomes. The nucleosomes were assembled on core 147-bp DNA segments and we used excess nucleosomes over remodeling enzymes. The magnitude of the differences in ATPase rates is small (at most threefold) and shows no correlation with nucleosome stability (Table 1). This suggests that RSC and ACF are able to reposition nucleosomes assembled on all test sequences using similar amounts of ATP.

Together, the above results indicate that DNA sequence does not regulate the activity of ATP-dependent chromatin remodeling complexes by changing nucleosome stability. We next investigated if a particular curved DNA sequence can inhibit remodeling activity.

A highly curved sequence element does not alter remodeling rate or binding affinity by ACF

It has recently been suggested that the activity of ACF may be regulated in a sequence-specific manner. It was hypothesized that a particular 40-bp stretch of DNA with a high degree of intrinsic curvature, when positioned over the nucleosomal dyad, adopts a conformation on the nucleosome that is incompatible with ACF binding.[15] In this model, the ACF-catalyzed remodeling of nucleosomes containing this sequence results in an accumulation of nucleosomes with the 40-bp segment aligned with the dyad because these nucleosomes cannot be bound by ACF.

To dissect out the effect of the 40-bp element on ACF remodeling, we designed a construct in which the 40-bp curved element replaced the central 40 bp of the 601 sequence (Fig. 4a). Insertion at this location is theoretically predicted to maintain the continuous curvature present in the 601 sequence (Supplementary Fig. 1). Despite this alignment, insertion of the 40-bp element slightly increased the proportion of alternative nucleosome positions (Fig. 4b). However, the majority of the nucleosomes (>75% relative to 601) were still positioned at one end of the DNA corresponding to the starting substrate for the reaction (Fig. 4b and see Materials and Methods). We first tested if the presence of this sequence affected the rate of remodeling by ACF under multiple turnover conditions. In these experiments, a limiting amount of ACF was used to remodel excess and saturating amounts of nucleosomes. These conditions reflect an *in vivo* situation where DNA sequence can influence recruitment. The two types of nucleosomes were labeled with different fluorescent dyes. ACF remodels both types of end-positioned nucleosomes with very similar rates (Fig. 4b, top, and c, left). We obtain a similar

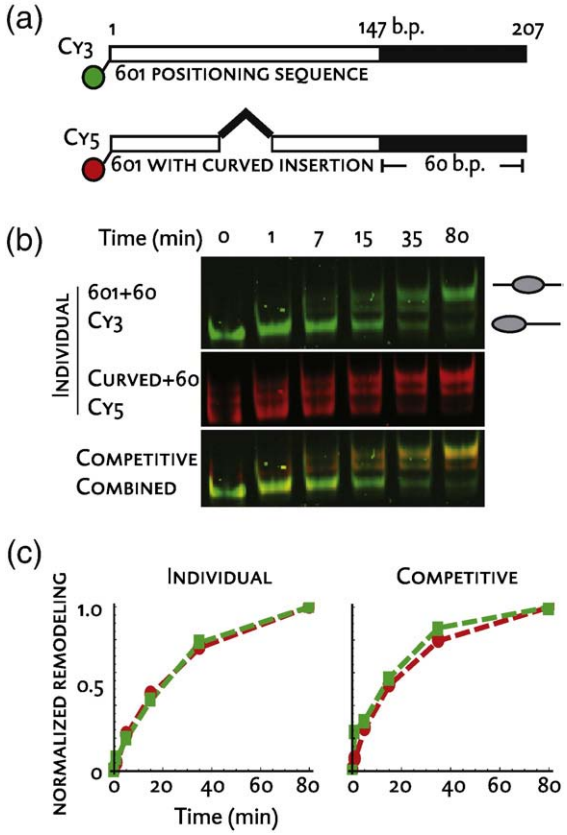

Fig. 4. Curved sequence does not affect remodeling rate or binding affinity of remodeling enzyme. (a) Schematic of constructs used for remodeling assay. Fluorophores are used to discriminate nucleosomes in single reaction mix. The 40-bp curved element is inserted in the middle of the 601 positioning sequence so that it aligns with the dyad in the end-positioned nucleosome. There are an additional 60 bp beyond the 601 sequence to allow movement of the nucleosome. (b) Upshift gel shows ACF (15 nM) centers nucleosomes assembled on both constructs under multiple turnover conditions at similar rates. The top two panels represent separate reactions with individual nucleosomes (80 nM each). In the bottom panel, the colors are merged to depict data from a single reaction with mixed nucleosomes (40 nM each, combined). (c) Quantification of data from (b). Left, individual reactions; right, competitive reaction.

result when the 40-bp element is placed within centered nucleosomes (Supplementary Fig. 3). Together, these results indicate that the presence of the 40-bp element within nucleosomes does not slow remodeling by ACF once ACF is fully bound.

To investigate if the 40-bp element reduced binding by ACF, we used the same set of nucleosomes in a competitive remodeling experiment. Equal concentrations of nucleosomes with and without the curved element were mixed with a limiting amount of ACF.[35] The different fluorescent labels on each type of nucleosome allowed us to visualize their remodeling separately (Fig. 4b). Under these competitive conditions, ACF should partition between the two nucleosomes based on their relative binding affinities. The observed remodeling rates for the two types of nucleosomes then reflect both the binding preference and the remodeling preference that ACF has for either type of nucleosome. Because ACF does not show a remodeling preference (Fig. 4b, top two panels, and c, left panel), any observed difference in rates under competitive conditions would reflect a difference in the binding preference of ACF. We find that ACF remodels both types of nucleosomes with similar rates under these competitive conditions. This indicates that the 40-bp element does not inhibit binding by ACF (Fig. 4c).

Outcome of remodeling reaction is determined by sequence on local level

The above results raise the strong possibility that DNA mainly influences remodeling by influencing the collapse of remodeling intermediates into specific nucleosomal locations. We tested this possibility in the context of ACF because unlike RSC, ACF generates only canonical nucleosomes. This allows us to more clearly visualize any differences in final nucleosome positions. We also used a longer nucleosome construct for two related reasons: (i) it has previously been reported that local positioning differences in the products are not easily visualized by native gel when the DNA fragment is on the order of 200 bp[14] and (ii) on DNA constructs shorter than 250 bp, the DNA length sensing mechanism of ACF is expected to drive nucleosomes to a narrowly clustered set of centrally positioned nucleosomes, as seen in Fig. 3f and described previously.[18]

We compared the outcome of ACF remodeling on two 347-bp constructs. Both constructs have a 601 sequence at one end to localize the starting nucleosome position. Unlike the experiment in Fig. 4, the 40-bp sequence is not inserted within the 601 sequence. In this case, one construct contains the 40-bp curved DNA element in the center of the 347-bp sequence (Fig. 5a). Using this longer nucleosomal construct, we observe many different remodeled products that migrate more slowly than the starting nucleosome. The presence of the 40-bp element significantly changes the final distribution of products (Fig. 5b and c). The differences in outcome are not due to an incomplete reaction, as the product distributions did not change with longer times (data not shown).

The data in Fig. 5 are analogous to previous observations that the 40-bp element alters the final locations of the nucleosomes remodeled by ACF.[15] Previously, this ability of the 40-bp element to change the positions of remodeled nucleosomes was hypothesized as arising from an inhibitory effect on ACF binding.[15] The results from Fig. 4 rule out an effect of the 40-bp element on ACF binding and together with the results from Fig. 5 and thermodynamic modeling of the resulting positions (Supplementary Fig. 2) suggest an alternative model: DNA sequence does not directly affect remodeling activity but rather helps direct the rotational setting

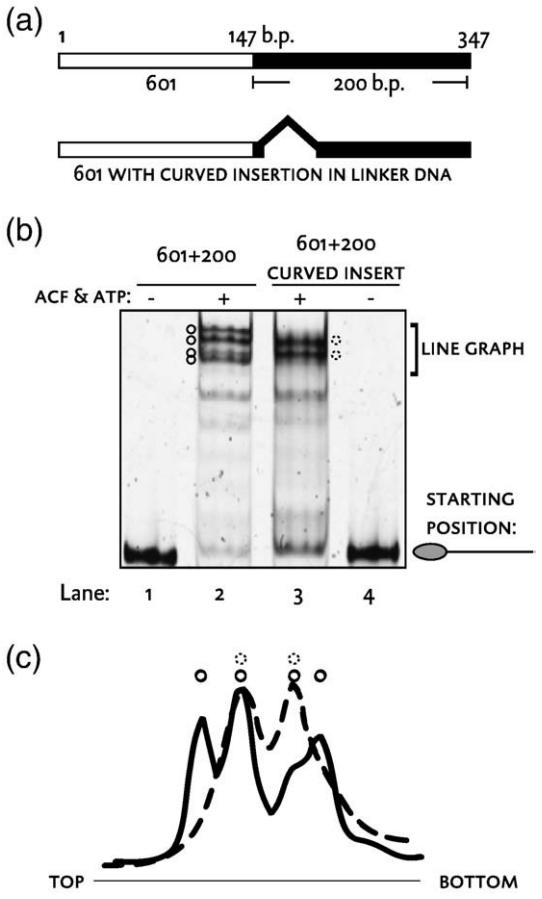

Fig. 5. Sequence affects positioning outcome. (a) Schematic of constructs used for remodeling assay. A 40-bp curved element is inserted in the middle of a 601 + 200 sequence to test whether it will influence distribution of nucleosome positions after remodeling. Longer flanking DNA allows for better visualization of alternate positions. (b) Comparing final positions of nucleosomes assembled on 600 + 200 (lane 2) with those assembled on the sequence containing the curved element (lane 3) shows a different distribution of final positions. The initial population for nucleosomes assembled on both constructs is homogenously end-positioned (lanes 1 and 4). (c) Line graphs of the region of difference shows that incorporation of curved element influences final distribution of products (lane 2, continuous line, *versus* lane 3, dashed line).

adopted by a remodeled nucleosome once it is released by the remodeling enzyme.

Discussion

ATP-dependent chromatin remodeling enzymes change the accessibility of DNA and alter transcriptional programs by directing nucleosomes to new positions. Here we analyze how the underlying DNA sequence influences ATP-driven transitions between different chromatin states. As it had already been shown that histone–DNA affinity can alter the rates of thermal repositioning,[8,13] we first considered the simple hypothesis that increasing the affinity between the histones and DNA would also slow nucleosome repositioning by remodeling enzymes. By comparing the remodeling activities of two major classes of remodeling complexes on a series of nucleosomal templates controlled for DNA length, we found that variation of the affinity of histones for DNA did not affect the rates of remodeling. We next addressed whether the presence of a DNA sequence with strong intrinsic curvature properties could affect remodeling activity. It had previously been hypothesized that a particular highly curved 40-bp sequence, when present within a nucleosome, inhibits binding by ACF and thereby helps stabilize nucleosomes in specific locations. By directly measuring ACF activity on nucleosomes containing this sequence, we found that the 40-bp sequence does not affect nucleosome remodeling or binding by ACF. The sequence, however, does affect the preferred local positions adopted by the remodeled nucleosomes, consistent with previous observations.[15] We discuss the mechanistic and broader biological implications of these findings below.

Mechanistic implications

Our observation that varying the strength of the binding interface between the histones and nucleosomal DNA does not affect the rates of remodeling most simply suggests that disrupting histone–DNA interactions is not rate-limiting during the overall remodeling reaction.[49] Previous work has shown that both the ISWI class and SWI/SNF class of chromatin remodeling enzymes can translocate on DNA,[36,37] and it has been proposed that this activity is critical for displacing the DNA from histones. It is therefore possible that the energetically most costly and, consequently, the slowest step of the remodeling reaction is translocation of the enzyme on nucleosomal DNA, or analogously, that a conformational rearrangement in the remodeling enzyme required for activation is the slowest step.

Further, it is possible that the energy from the amount of ATP used by the enzyme is sufficient to substantially lower the activation energy for breaking the strongest histone-DNA contacts tested. For reference, the free energy released from hydrolysis of one ATP molecule under physiological conditions is greater than the free energy required to completely dissociate half of the histone-DNA contacts on a 601 nucleosome.[30,31] In addition, it has been speculated that the step size of ATP-dependent chromatin remodeling complexes is of the order of 10 bp,[18,19,38] in which case, the energy from one ATP hydrolysis event, if used efficiently, will be more than sufficient.

The data presented in this work lead to the question of how the activity of the enzyme can remain unaffected by changes in DNA sequence, while the outcome of the remodeling reaction is altered[14] (Fig. 5). A sequence-dependent outcome in the context of sequence-independent activity can be explained if DNA sequence influences the collapse of a high-energy intermediate generated by enzyme action into highly resolved nucleosome positions (Fig. 6a). Our model conceptually divides the remodeling reaction into two components—local guidance based on sequence interaction with nucleosome *versus* global (or long-range) guidance by the remodeler. We first present a model based on the physical properties of the nucleosome for how DNA sequence can locally direct nucleosome locations (Fig. 6b–d) and then discuss implications for the regulation of the enzyme within an *in vivo* context.

Effects of sequence on local nucleosome positions

When assembled into a nucleosome, DNA adopts a high degree of curvature relative to the persistence length of DNA. The energetic cost of loop formation is balanced by the energy gained through forming 12 discrete contacts between histones and the DNA backbone.[39,40] There are no base-pair-specific contacts between the histones and the DNA, so the base pair composition of a sequence is thought to influence affinity for the nucleosome only to the extent that it dictates its propensity and ability to curve around the histone octamer.[6,7]

Since the DNA molecule has a helical structure with an ~10-bp repeat, the groove facing the nucleosome alters every 5 bp (Fig. 6b). Correspondingly, it has been shown that sequences that contain 10-bp spaced repeats of AT and GC dinucleotides with 5-bp relative offsets preferentially bind nucleosomes. This is because every 10-bp AT/TT/TA dinucleotide provides a favorable local structure for compression of the minor groove, while a 5-bp offset of GC dinucleotides lowers the energetic cost of compression of the corresponding major groove when it faces the nucleosome core.[21,24,25] Such an arrangement of dinucleotides confers a handedness to the bend of the DNA molecule such that the direction of curvature of the DNA is aligned with the curvature of the histone octamer.

Consider the effect of a 10-bp translation of such a sequence relative to the histone octamer on the overall free energy of the complex. Given the ~10-bp helical periodicity, such a translation would retain the alignment between the handedness of the DNA curvature and the octamer, while maintaining the discrete points of contact. So, the change in

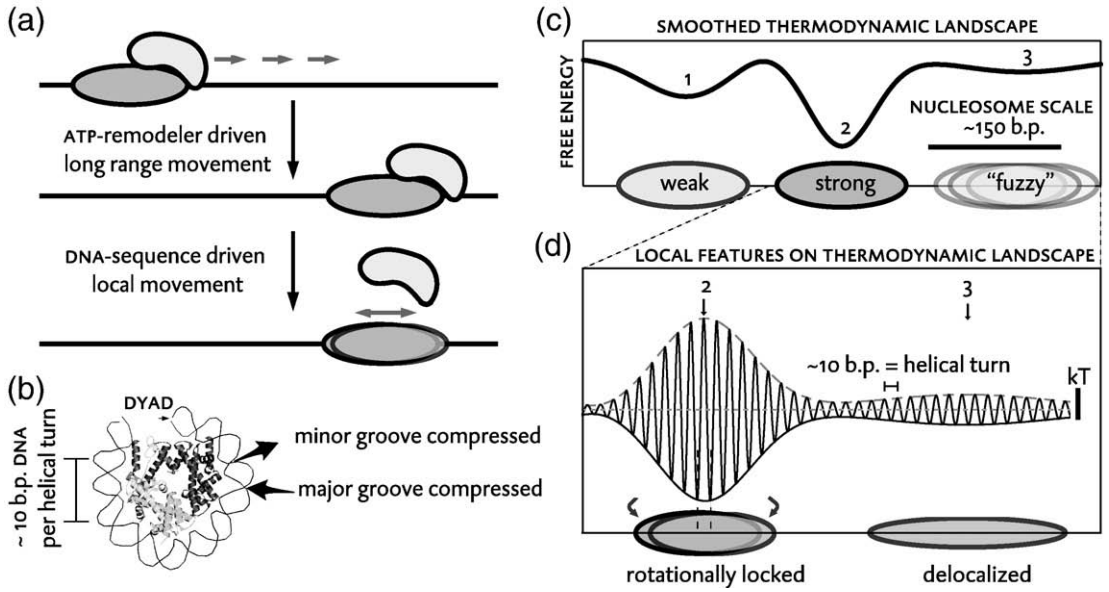

Fig. 6. Model: Sequence and remodelers cooperate to achieve positioning outcome. (a) Model of cooperation between remodeling enzymes and sequence. Remodeling enzymes move nucleosomes over large distances in a sequence-independent manner, but sequence influences local settling of remodeling intermediate to give a final stable state. (b) Structure of one-half of the nucleosome shows that DNA is highly bent around the histone octamer. In this bent structure, within the helical turn (~10 bp), DNA compression alternates between the major and minor groove every 5 bp. If nucleosome affinity is determined by a correspondence of the intrinsic curvature of the sequence and the curvature dictated by the physical constraints of the nucleosome, then a translation of the DNA relative to the nucleosome by 5 bp would also flip the rotational orientation of the DNA, pairing the two curvatures in opposition, and result in a highly unfavorable sequence. (c) Schematic of three kinds of positioning wells on a smooth thermodynamic affinity landscape. (1) A shallower well corresponds to lower stability and/or lower occupancy. (2) A strong positioning sequence corresponds to a stable energy well. (3) Broad or ambiguous energy wells correspond to delocalized or "fuzzy" nucleosomes. (d) Model for how the bending preference of the DNA sequence imposes local features on the thermodynamic landscape. Regions corresponding with wells 2 and 3 from (c) are chosen for contrast and a continuous distribution of curvature is assumed to model local features in this schematic. The bottom track depicts the fate of two nucleosomes released by the remodeler at positions indicated by the numbered arrows. The energetic barriers between adjacent rotational positions (designated based on the location of the dyad) are depicted as being greater than thermal energy (kT, black scale bar) for the central positions of well 2 and depicted as comparable to thermal energy in well 3. A nucleosome released near the center of well 2 will be kinetically trapped into a local cluster of rotationally phased positions. Local clustering is observed for the majority of nucleosomes in yeast genome.[1] A nucleosome released at the center of well 3 will not experience significant kinetic barriers in moving between adjacent rotational settings and would occupy a wide distribution of rotational and translational positions (delocalized or fuzzy nucleosomes), as is observed for a minority of yeast nucleosomes.[1] Local rotational clustering can also be mediated solely thermodynamically (not shown here). In this case, certain rotational positions will have substantially greater stability than neighboring positions, and the energetic barriers between adjacent rotational positions will be less than kT, allowing rapid equilibration.

overall affinity would be mostly attributable to the difference of the contributions from the departing and arriving 10 bp. In contrast, a translation of such a sequence by half a helical turn (5 bp) would disrupt the correspondence between the preferred helical handedness of the DNA and the curvature of the nucleosome, resulting in a highly unstable position.

These local features of an energy landscape are represented in Fig. 6d for an idealized sequence of continuously distributed intrinsic curvature. This representation of the thermodynamic landscape is consistent with two properties of nucleosome positions *in vivo*; that many nucleosomes occupy highly resolved positions, and that nucleosomes tend to cluster at 10-bp offsets.[4] A smooth energy landscape as in Fig. 6c would correspond to a smooth probability distribution of nucleosome locations. In contrast, by analogy to the combination of positive and negative feedback to achieve higher precision in many biological control systems, the close interspersion of high- and low-affinity rotational registers (Fig. 6d) can achieve higher positioning precision. The distribution of bending properties may be periodic, as schematized in Fig. 6d, or nonperiodic. A nonperiodic distribution of bending properties within a sequence can give rise to irregular thermodynamic landscapes with varying well depths and barrier heights. This is suggested for the 40-bp element, the presence of which introduces nonuniform changes in the predicted thermodynamic landscape of nucleosome positions (Supplementary Fig. 2).

We hypothesize that the height of the peak that separates two wells representing adjacent rotational settings (Fig. 6d) reflects the activation energy required for the nucleosome to switch between the two settings. This hypothesis is based on the

assumption that switching requires transition through the intermediate rotational setting represented by the peak separating the two adjacent wells.

When the energetic difference between the peaks and wells is less than thermal energy (less than kT (k refers to the Boltzmann constant and T refers to the temperature in degrees Kelvin. kT is a measure of thermal energy), ~0.6 kcal/mol), a nucleosome would rapidly equilibrate among adjacent rotational settings and the relative depths of the wells would determine the overall distribution of positions. In contrast, when differences between the peaks and wells are much greater than kT, equilibration between adjacent rotational settings would be slow on a physiological time scale, and nucleosomes would get kinetically trapped in certain rotational settings. Conceivably high peaks can then result in sharply defined rotational positions even in the context of shallow wells. This model extends the definition of a strong positioning sequence to incorporate the height of kinetic energy barriers between neighboring rotational positions, in addition to the overall sequence affinity (Fig. 6d). Previous theoretical calculations suggest that the energetic barrier between neighboring nucleosome positions separated by 5 bp can span a large range depending on sequence. Calculations for *Kluyveromyces lactis* centromeric DNA sequences suggest that this local barrier can be as large as 15 kcal/mol,[41] while similar calculations for human telomeric DNA sequences suggest that the barrier is negligible compared to thermal energy.[42]

Global action of remodeler

We have shown that the thermodynamic stability of nucleosomes does not regulate the efficiency of two key chromatin remodeling enzymes, RSC and ACF. Rather, our data with ACF suggest that the intrinsic remodeling mechanism dictates long-range translational shifts, while the local nucleosome positioning landscape resolves the final position and rotational phase. Indeed, substantial previous work has shown that, on the same DNA sequence, different remodeling enzymes relocate nucleosomes to distinct translational positions as a result of intrinsic mechanistic differences.[9,11,14] We hypothesize that consequent to remodeling, the DNA sequence promotes the collapse of a high-energy remodeled intermediate into a particular set of stable nucleosomal positions. *In vivo*, the available positions will be further restricted by neighboring nucleosomes, other DNA bound factors, and the state of chromatin compaction.

The capacity of chromatin remodeling enzymes to remodel sequences of variable affinity at similar rates casts them as versatile molecular machines capable of preserving their specific function once recruited to any locus. This versatility with respect to the nucleosomal DNA sequence is consistent with substantial previous work, suggesting that a large part of the specificity of remodeling enzymes arises from targeting via sequence-specific DNA binding factors and factors that recognize specific histone modifications.[11,43,50] Significantly, ACF and RSC act globally at a diverse set of genomic loci dependent on cellular state and participate in different functional pathways. Moreover, a key homolog of ACF in yeast, the Isw2 complex, has been observed to directionally slide a nucleosome *in vivo* across low-affinity dA–dT-rich sites shown to repel nucleosomes.[44]

Conclusion

Many nucleosomes occupy highly defined and reproducible positions in vivo, either at the level of single base pairs, or at the level of 10-bp rotational phases. While such 10-bp phasing could simply reflect the stochastic consequence of the dominant mode of curvature distribution within natural positioning sequences, recent work implies that the precise rotational position of the nucleosome has functional significance. This argument is based on observations that shifts in nucleosome positions by a few base pairs can have a profound impact on transcription[45] and by the observation that transcription factors show preferential alignments on the surface of the nucleosome with helical periodicity.[4] Intriguingly, nucleosome-bound sequences within regulatory regions exhibit selection against mutations that disrupt helical phase.[51]

Previous work has already revealed the potential of a sequence-dependent nucleosome positioning code. Our study suggests a mechanism by which the remodeler and sequence can cooperate to switch nucleosomes between two different locally meaningful positions based on environmental stimuli. We hypothesize that after providing the energy to overcome local kinetic barriers between neighboring positions, the remodeler releases the nucleosome in the general vicinity of a regulatory region, while the underlying DNA sequence directs the settling of the nucleosome into a functional rotational position. This collaboration between remodeling enzymes, which provide range, and DNA sequence, which provides precision, may allow nucleosomes to toggle between well-defined cellular state-dependent positions like clicks of a switch.

Materials and Methods

Protein purification

RSC was purified from *Saccharomyces cerevisiae* via a TAP tag attached to the Rsc2 subunit as described previously.[46] The human ACF complex was purified, assembled and purified from Sf9 cells via a FLAG tag attached to the SNF2h subunit as previously described.[18]

Nucleosome assembly

The 601, TPT, 5S and ARB positioning sequences were modified to contain a PstI site 18 bp in from one end. DNA constructs of different lengths were generated by PCR and

gel-purified. Specifically, for the FRET kinetics measurements, ACF gel mobility shifts, and ATPase experiments, test sequences included 60 bp of flanking DNA to accommodate movement of the nucleosome. The experiment in Fig. 5 required a longer construct with 200 flanking base pairs, and other experiments (Figs. 2 and 3c) were done on 147-bp sequences without any flanking DNA, as described in the text and figures. Cy3- or Cy5-labeled DNA was generated by PCR using end-labeled primers (IDT). (Primer sequences are available upon request.) DNA fragments were assembled into mononucleosomes with recombinant *Xenopus* histones using the gradient salt dialysis method.[47] Nucleosomes used in the FRET kinetics experiment were assembled on octamers containing H2A labeled with Cy5 at residue 120, as described. [18] For 5S, TPT and ARB positioning sequence containing nucleosomes, we enriched for end-positioned nucleosomes by glycerol-gradient purification.[47]

Competitive assemblies

In this method developed by Shrader and Crothers[24,25] and further optimized by Lowary and Widom,[21,26] labeled tracer DNA competes with a large excess of unlabeled competitor DNA for limiting amounts of histone octamer. The referenced method was used with slight modification. Tracer amounts of Cy3-labeled 147-bp core DNA fragments of each test sequence were mixed with 40 μg of ARB core DNA serving as background. Both were competing for 3 μg of octamer in a 60-μl reaction containing 20 mM Tris–HCl (pH 7.7), 10 mM DTT, and 0.5 mM benzamidine. The reaction was gradually dialyzed at 4 °C from high-salt-concentration 2 M NaCl into TE buffer using an established assembly method shown to yield equilibrium measurements.[21,26] Reconstitution reactions were repeated multiple times on different days. Measurements were further validated by repetition with different background DNA (30 μg 5S, not shown.). The assembled reactions were run on 0.5× TBE [tris–borate–EDTA (ethylenediaminetetraacetic acid)] nondenaturing 5% (v/v) polyacrylamide gels. Tracer DNA was visualized by scanning on a Typhoon Variable Mode Imager (GE Healthcare) with the Cy3 filter set, while total DNA was similarly visualized using SYBR gold staining (Invitrogen). ImageQuant (GE Healthcare) was used to quantify band intensities.

For a competitive assembly reaction with a given tracer sequence represented by "D", an equilibrium constant (K_{eq}^{D}) was calculated from the molar ratio of nucleosomes to free DNA. An equilibrium constant was also obtained using the background sequence, ARB, as a tracer (K_{eq}^{ARB}). The relative free energies were then obtained from Eq. (1) for 4 °C.

$$\Delta\Delta G_{ARB} = -RT\ln\left(K_{eq}^{D}/K_{eq}^{ARB}\right) \quad (1)$$

where R is the gas constant and T is the temperature.

For consistency, the $\Delta\Delta G$ values calculated from the site exposure values are also reported relative to ARB.

Proper equilibration was indicated by the value of K_{eq}^{ARB}. This value is obtained under conditions where the tracer and background sequences are identical and therefore should be equal to the molar ratio of octamer to background DNA. This ratio should also be equal for all reactions when total DNA is quantified. The variability of this ratio across all test conditions within a single dialysis experiment was used to calculate global experimental error (±0.05 kcal/mol) and can be interpreted as the uncertainty of the ARB sequence, otherwise defined as 0 (see Table 1).

FRET experiments

FRET-based remodeling reactions contained either 25 nM ACF or 40 nM RSC. All reactions contained 10 nM nucleosomes (assembled on various sequences as reported) in reaction buffer: 20 mM Tris–HCl (pH 7.7), 60 mM KCl, 10% glycerol and 3 mM free Mg^{2+}. Reactions were initiated by the addition of 4 μM ATP at 30 °C. Both RSC and ACF activity under saturating ATP conditions is on a time scale too fast to be accurately measured by our FRET-based method. We therefore used a subsaturating ATP concentration of 4 μM to be able to follow the entire time course. FRET-based kinetics data were collected on an ISS K2 fluorimeter.[18] The data were fit to two exponentials using MATLAB (Mathworks). The rate constants reported in Table 1 are for the first fast phase. The second slower phase is thought to represent a small population of nucleosomes that get remodeled more slowly, as explained previously.[18] Values reported in table are averaged across $n > 3$ conditions, with error reported as SEM from a pool of individual runs with typical R values of >0.99 to the fit.

ACF gel mobility shift experiments

All the ACF reactions analyzed by gel mobility shift were performed in the same basic buffer conditions as above with variations in ACF, nucleosome and ATP concentrations as described below. All reactions were stopped with 2× stop buffer (115 mM ADP, 0.8 mg/ml unrelated stop plasmid DNA to compete off the enzyme) and run on a 0.5× TBE nondenaturing 5% (v/v) polyacrylamide gel. The ACF reactants and products were visualized by scanning the gel on a Typhoon Variable Mode Imager (GE Healthcare) after SYBR gold staining (Invitrogen). The reactions in Fig. 3f were carried out with the same ACF and ATP concentrations as used in the FRET experiments. The reactions in Fig. 5b contained 25 nM ACF, 10 nM nucleosomes and 2 mM ATP–Mg^{2+}. We confirmed that these reactions had gone to completion by longer incubations and by controlling for time-dependent loss of enzyme activity and ATP depletion.

For limiting enzyme conditions used in the competition experiments (Fig. 4b), 15 nM ACF and a saturating concentration of 80 nM total nucleosome were used based on previous work[35] (and data not shown). Three reactions were run in parallel. The individual reactions (Fig 4b, top two panels, respectively) contained either (1) 80 nM of nucleosomes assembled on 601 + 60 sequence end-labeled with Cy3 or (2) 80 nM of nucleosomes assembled on 601 + 60 sequence containing the 40-bp curved insert in the center of 601 and end-labeled with Cy5 dye. The third condition (3) combined 40 nM of each nucleosome for a final concentration of 80 nM. The nucleosomes were visualized by scanning the gels on the Typhoon using the appropriate filters to visualize either the Cy3 or the Cy5 dyes. ImageQuant (GE Healthcare) was used to quantify band intensities, which were used to calculate the fraction of end-positioned (i.e., unremodeled) nucleosomes relative to all positions as a function of time and these were then normalized to time zero to obtain the normalized fraction of unremodeled nucleosomes [fr(U)]. The data in Fig. 4C represent [1 − fr(U)] plotted *versus* time.

Reported results are representative across three experiments conducted on different days.

Analysis of equilibrium constants for site exposure

We adapted a previous restriction enzyme accessibility approach pioneered by the Widom laboratory.[7,31] We measured the initial rates of cutting at a PstI site located 18 bp in from the end of different core nucleosomes. Restriction enzymes can cut nucleosomal DNA when it transiently unravels from the histone octamer. The rate of cutting by the highest achievable restriction enzyme concentrations is significantly slower than the rate at which the unraveled DNA rebinds the histone octamer.[48] As a result, cutting of nucleosomal restriction enzymes is slowed down relative to cutting of free DNA by a factor equal to the equilibrium constant for unraveling the amount of DNA required to expose the restriction site. As described previously, we obtained the equilibrium constants for unraveling nucleosomal DNA (K_{eq}^{conf}) by taking the ratio of the rate of cutting on a nucleosome to the rate of cutting on the corresponding free DNA sequence. The values in Table 1 are $\Delta\Delta G$ values calculated for 30 °C from differences between the given sequence and ARB for consistency and ease of comparison with the competition assembly values [Eq. (2)].

$$\Delta\Delta G_{ARB} = -RT\ln\left(K_{eq}^{conf}[ARB]/K_{eq}^{conf}[D]\right) \quad (2)$$

where D is the test sequence.

Reactions were initiated by addition of 10 U/μl PstI to 20 nM nucleosomes assembled on core segments of test sequences in a reaction buffer containing: 20 mM Tris–HCl (pH 7.7), 60 mM KCl, 5% glycerol and 3 mM free Mg^{2+} at 37 °C. Aliquots were removed at various times and quenched in 1.5 volumes of 10% glycerol, 70 mM EDTA, 20 mM Tris (pH 7.7), 2% SDS, 0.2 mg/ml xylene cyanole and bromophenol blue. Cut DNA was separated from uncut DNA on a 12% native polyacrylamide gel (1× TBE) after deproteinizing at 37 °C for 1 h with 1 mg/ml proteinase K. The DNA was visualized using a Typhoon after staining with SYBR gold. For each time point, the fraction of uncut *versus* cut DNA was quantified. Initial rates were obtained by fitting the first 10% of the reaction to a straight line.

RSC remodeling kinetics by restriction enzyme accessibility

Reactions containing 40 nM RSC, 10 nM nucleosomes, 3 mM free Mg^{2+} at 30 °C, and 0.2 U/μl PstI were initiated by the addition of 2 mM ATP–Mg^{2+}. Reactions were stopped, separated, visualized and quantified as in the above section. Rate constants were obtained by application of a first-order fit to the change in the fraction of uncut DNA as a function of time using MATLAB based on a previously established method.[34]

ATPase reactions

For reactions with ACF, 20 nM enzye and 80 nM nucleosomes were mixed in 20 mM Tris–HCl (pH 7.7), 60 mM KCl, 10% glycerol and 3 mM free Mg^{2+}. RSC reactions contained 1 nM RSC and 40 nM nucleosome in the same buffer. Experiments were initiated by the addition of 4 μM ATP containing trace amounts of [γ-^{32}P] ATP. Reactions were quenched, processed and quantified as described.[34]

Acknowledgements

We thank J. Widom for the 601 plasmid, J. J. Hayes for the 5S plasmid, C. Rowe for purified RSC and L. Racki for purified ACF enzyme. We thank J. Widom, S. Lomvardas and members of the Narlikar laboratory for helpful comments on the manuscript.

This work was supported by in part by grants from the NIH and the Beckman Foundation to G.J. N. P.D.P. is supported by an NSF Graduate Research Fellowship. G.J.N. is a Leukemia and Lymphoma Society Scholar.

Supplementary Data

Supplementary data associated with this article can be found, in the online version, at doi:10.1016/j.jmb.2009.04.085

References

1. Lee, W., Tillo, D., Bray, N., Morse, R. H., Davis, R. W. & Nislow, C. (2007). A high-resolution atlas of nucleosome occupancy in yeast. *Nat. Genet.* **39**, 1235–1244.
2. Shivaswamy, S., Bhinge, A., Zhao, Y., Jones, S., Hirst, M. & Iyer, V. R. (2008). Dynamic remodeling of individual nucleosomes across a eukaryotic genome in response to transcriptional perturbation. *PLoS Biol.* **6**, e65.
3. Segal, E., Fondufe-Mittendorf, Y., Chen, L., Thåström, A., Field, Y., Moore, I. *et al.* (2006). A genomic code for nucleosome positioning. *Nature*, **442**, 772–778.
4. Albert, I., Mavrich, T. N., Tomsho, L. P., Qi, J., Zanton, S. J. *et al.* (2007). Translational and rotational settings of H2A. Z nucleosomes across the *Saccharomyces cerevisiae*. *Nature*, **446**, 572–576.
5. Yuan, G., Liu, Y., Dion, M. F., Slack, M. D., Wu, L. F., Altschuler, S. J. & Rando, O. J. (2005). Genome-scale identification of nucleosome positions in *S. cerevisiae*. *Science*, **309**, 626–630.
6. Anselmi, C., Bocchinfuso, G., De Santis, P., Savino, M. & Scipioni, A. (2000). A theoretical model for the prediction of sequence-dependent nucleosome thermodynamic stability. *Biophys. J.* **79**, 601–613.
7. Widom, J. (2001). Role of DNA sequence in nucleosome stability and dynamics. *Q. Rev. Biophys.* **34**, 269–324.
8. Pisano, S., Marchioni, E., Galati, A., Mechelli, R., Savino, M. & Cacchione, S. (2007). Telomeric nucleosomes are intrinsically mobile. *J. Mol. Biol.* **369**, 1153–1162.
9. Narlikar, G. J., Fan, H. Y. & Kingston, R. E. (2002). Cooperation between complexes that regulate chromatin structure and transcription. *Cell*, **108**, 475–487.
10. Shivaswamy, S. & Iyer, V. R. (2008). Stress-dependent dynamics of global chromatin remodeling in yeast: dual role for SWI/SNF in the heat shock stress response. *Mol. Cell. Biol.* **28**, 2221–2234.
11. Smith, C. & Peterson, C. (2004). ATP-dependent chromatin remodeling. *Curr. Top. Dev. Biol.* **65**, 115–148.
12. Whitehouse, I., Rando, O. J., Delrow, J. & Tsukiyama, T.

(2007). Chromatin remodelling at promoters suppresses antisense transcription. *Nature*, **450**, 1031–1035.
13. Flaus, A. & Richmond, T. J. (1998). Positioning and stability of nucleosomes on MMTV 3′LTR sequences. *J. Mol. Biol.* **275**, 427–441.
14. Stockdale, C., Flaus, A., Ferreira, H. & Owen-Hughes, T. (2006). Analysis of nucleosome repositioning by yeast ISWI and Chd1 chromatin remodeling complexes. *J. Biol. Chem.* **281**, 16279–16288.
15. Rippe, K., Schrader, A., Riede, P., Strohner, R., Lehmann, E. & Längst, G. (2007). DNA sequence- and conformation-directed positioning of nucleosomes by chromatin-remodeling complexes. *Proc. Natl Acad. Sci. USA*, **104**, 15635–15640.
16. Sims, H. I., Baughman, C. B. & Schnitzler, G. (2008). Human SWI/SNF directs sequence-specific chromatin changes on promoter polynucleosomes. *Nucleic Acids Res.* **36**, 6118–6131.
17. Sims, H. I., Lane, J. M., Ulyanova, N. P. & Schnitzler, G. R. (2007). Human SWI/SNF drives sequence-directed repositioning of nucleosomes on C-myc promoter DNA. *Biochemistry*, **40**, 11377–11388.
18. Yang, J. G., Madrid, T. S., Sevastopoulos, E. & Narlikar, G. J. (2006). The chromatin-remodeling enzyme ACF is an ATP-dependent DNA length sensor that regulates nucleosome. *Nat. Struct. Mol. Biol.* **13**, 1078–1083.
19. Zofall, M., Persinger, J., Kassabov, S. & Bartholomew, B. (2006). Chromatin remodeling by ISW2 and SWI/SNF requires DNA translocation inside the nucleosome. *Nat. Struct. Mol. Biol.* **13**, 339–346.
20. Kang, J. G., Hamiche, A. & Wu, C. (2002). GAL4 directs nucleosome sliding induced by NURF. *EMBO J.* **21**, 1406–1413.
21. Lowary, P. T. & Widom, J. (1998). New DNA sequence rules for high affinity binding to histone octamer and sequence-directed nucleosome positioning. *J. Mol. Biol.* **276**, 19–42.
22. Schnitzler, G., Sif, S. & Kingston, R. E. (1998). Human SWI/SNF interconverts a nucleosome between its base state and a stable remodeled state. *Cell*, **94**, 17–27.
23. Hayes, J. J. & Wolffe, A. P. (1993). Preferential and asymmetric interaction of linker histones with 5S DNA in the nucleosome. *Proc. Natl Acad. Sci. USA*, **90**, 6415–6419.
24. Shrader, T. E. & Crothers, D. M. (1989). Artificial nucleosome positioning sequences. *Proc. Natl Acad. Sci. USA*, **86**, 7418–7422.
25. Shrader, T. E. & Crothers, D. M. (1990). Effects of DNA sequence and histone–histone interactions on nucleosome placement. *J. Mol. Biol.* **216**, 69–84.
26. Lowary, P. T. & Widom, J. (1997). Nucleosome packaging and nucleosome positioning of genomic DNA. *Proc. Natl Acad. Sci. USA*, **94**, 1183–1188.
27. Thåström, A., Lowary, P. T. & Widom, J. (2004). Measurement of histone–DNA interaction free energy in nucleosomes. *Methods*, **33**, 33–44.
28. Li, G. & Widom, J. (2004). Nucleosomes facilitate their own invasion. *Nat. Struct. Mol. Biol.* **11**, 763–769.
29. Längst, G. & Becker, P. B. (2004). Nucleosome remodeling: one mechanism, many phenomena? *Biochim. Biophys. Acta*, **1677**, 58–63.
30. Polach, K. J. & Widom, J. (1995). Mechanism of protein access to specific DNA sequences in chromatin: a dynamic equilibrium model for gene regulation. *J. Mol. Biol.* **254**, 130–149.
31. Anderson, J. D., Thastrom, A. & Widom, J. (2002). Spontaneous access of proteins to buried nucleosomal DNA target sites occurs via a mechanism that is distinct from nucleosome translocation. *Mol. Cell. Biol.* **22**, 7147.
32. Ito, T., Bulger, M., Pazin, M. J., Kobayashi, R. & Kadonaga, J. T. (1997). ACF, an ISWI-containing and ATP-utilizing chromatin assembly and remodeling factor. *Cell*, **90**, 145–155.
33. Eberharter, A., Ferrari, S., Längst, G., Straub, T., Imhof, A., Varga-Weisz, P., Wilm, M. & Becker, P. B. (2001). Acf1, the largest subunit of CHRAC, regulates ISWI-induced nucleosome remodelling. *EMBO J.* **20**, 3781–3788.
34. Narlikar, G. J., Phelan, M. & Kingston, R. E. (2001). Generation and interconversion of multiple distinct nucleosomal states as a mechanism for catalyzing chromatin fluidity. *Mol. Cell*, **8**, 1219–1230.
35. Chang, E. Y., Ferreira, H., Somers, J., Nusinow, D. A., Owen-Hughes, T. & Narlikar, G. J. (2008). MacroH2A allows ATP-dependent chromatin remodeling by SWI/SNF And ACF complexes but specifically reduces recruitment of SWI/SNF. *Biochemistry*, **47**, 13726–13732.
36. Saha, A., Wittmeyer, J. & Cairns, B. R. (2002). Chromatin remodeling by RSC involves ATP-dependent DNA translocation. *Genes Dev.* **16**, 2120–2134.
37. Whitehouse, I., Stockdale, C., Flaus, A., Szczelkun, M. D. & Owen-Hughes, T. (2003). Evidence for DNA translocation by the ISWI chromatin-remodeling enzyme. *Mol. Cell. Biol.* **23**, 1935–1945.
38. Schwanbeck, R., Xiao, H. & Wu, C. (2004). Spatial contacts and nucleosome step movements induced by the NURF chromatin remodeling complex. *J. Biol. Chem.* **279**, 39933–39941.
39. Luger, K., Mäder, A. W., Richmond, R. K., Sargent, D. F. & Richmond, T. J. (1997). Crystal structure of the nucleosome core particle at 2.8 Å resolution. *Nature*, **389**, 251–260.
40. Scipioni, A., Pisano, S., Anselmi, C., Savino, M. & De Santis, P. (2004). Dual role of sequence-dependent DNA curvature in nucleosome stability: the critical test of highly bent *Crithidia fasciculata* DNA tract. *Biophys. Chem.* **107**, 7–17.
41. Mattei, S., Sampaolese, B., De Santis, P. & Savino, M. (2002). Nucleosome organization on *Kluyveromyces lactis* centromeric DNAs. *Biophys. Chem.* **97**, 173–187.
42. Filesi, I., Cacchione, S., De Santis, P., Rossetti, L. & Savino, M. (2000). The main role of the sequence-dependent DNA elasticity in determining the free energy of nucleosome formation on telomeric DNAs. *Biophys. Chem.* **83**, 223–237.
43. Fazzio, T. G., Gelbart, M. E. & Tsukiyama, T. (2005). Two distinct mechanisms of chromatin interaction by the Isw2 chromatin remodeling complex *in vivo*. *Mol. Cell. Biol.* **25**, 9165–9174.
44. Whitehouse, I. & Tsukiyama, T. (2006). Antagonistic forces that position nucleosomes *in vivo*. *Nat. Struct. Mol. Biol.* **13**, 633–640.
45. Martinez-Campa, C., Politis, P., Moreau, J. L., Kent, N., Goodall, J., Mellor, J. & Goding, C. R. (2004). Precise nucleosome positioning and the TATA box dictate requirements for the histone H4 tail and the bromodomain factor Bdf1. *Mol. Cell*, **15**, 69–81.
46. Wittmeyer, J., Saha, A. & Cairns, B. (2004). DNA translocation and nucleosome remodeling assays by the RSC chromatin remodeling complex. *Methods Enzymol.* **377**, 322–343.
47. Luger, K., Rechsteiner, T. J. & Richmond, T. J. (1999). Expression and purification of recombinant histones and nucleosome reconstitution. *Methods Mol. Biol. (Clifton, N. J.)*, **119**, 1–16.

48. Polach, K. J. & Widom, J. (1999). Restriction enzymes as probes of nucleosome stability and dynamics. *Methods Enzymol.* **304**, 278–298.
49. Johnson, D. S., Bai, L., Smith, B. Y., Patel, S. S. & Wang, M. D. (2007). Single-molecule studies reveal dynamics of DNA unwinding by the ring-shaped T7 helicase. *Cell*, **129**, 1299–1309.
50. Kouzarides, T. (2007). Chromatin modifications and their function. *Cell*, **128**, 693–705.
51. Sasaki, S., Mello, C. C., Shimada, A., Nakatani, Y., Hashimoto, S., Ogawa, M. *et al.* (2009). Chromatin-associated periodicity in genetic variation downstream of transcriptional start sites. *Science*, **323**, 401–404.